SUPPLEMENTARY MATERIALS AND METHODS

Tissue Sample Collection and Processing

Skin biopsies from depigmented skin of 6 untreated vitiligo patients (3 women and 3 men, between 34-66 years old) and from repigmented skin of 10 generalized active vitiligo patients (6 women and 4 men, between 8-70 years old) were collected from the trunk or limbs. All vitiligo patients had generalized vitiligo with >25% body surface affected. Treated patients received 0.5 J/cm^2 of NBUVB twice a week for 4 months. Only areas with complete clinical repigmentation were collected. We focused our biopsy collection on the trunk and limbs (including arms, forearms, thighs and calves) all being locations with a good density of hair follicles, where the perifollicular repigmentation was well observed. Collection was avoided from locations with low density or absent hair follicles, like ventral arms and forearms and acral sites. The biopsies were collected from the center of depigmented spots of untreated patients and from the center of repigmented spots, more than 5 mm apart from the lesion border. The presence in the biopsy of white hairs was avoided, and was ruled out for each hair follicle by checking in the studied transverse sections the positive expression of melanocyte (MC) markers at bulge and bulb. Biopsies from treated skin were taken from lesions of which diameter was larger than 6 mm. Because in our previous clinical work with vitiligo patients (2) we did not observe variation of repigmentation by age or gender, the studied vitiligo samples were not matched by age and gender. The biopsies before and during NBUVB treatment could not be paired, due to patient collection issues. The following criteria were used for patients enrollment: a. inclusion criteria: either male or female of skin type I-IV suffering from generalized active vitiligo, with ages between 7-80 years. Vitiligo

patients should have white patches occurred after birth on trunk and limbs with ≥25% body surface area involvement; b. exclusion criteria: use of phototherapy during the previous 2 years; use of any depigmenting agents (e.g. monobenzylether of hydroquinone or hydroquinone); vitiligo limited to the back of the hands, dorsum of the feet, face, genitalia, patients taking immunosuppressive drugs or corticosteroids by mouth or other route of administration; subjects with high sensitivity to sunlight; patients allergic to Lidocaine; women who are pregnant or may become pregnant during the course of the study; lactating women; subjects taking medications and herbal supplements that may increase a subject's sensitivity to the sun.

Normal control skin from six women was collected from the trunk. Controls were between 19-48 years old. Immediately after the biopsy, the skin samples collected were transported to the dermatology lab in RPMI. Untreated vitiligo, NBUVB-treated vitiligo and normal human skin samples were then embedded in OCT medium using transverse orientation, snap-frozen in liquid nitrogen within 20 minutes of collection, and stored at -80°C. Tissue cryosections 6 μM thick were cut under RNAse-free conditions and mounted on Aminosilane adhesive slides (Newcomer Supply) by the Morphology and Phenotyping Core at the University of Colorado. Slides were maintained at -80°C until use for LCM.

Hair Follicle Bulge Mapping

To map the hair follicle bulge in all of our tissue samples, frozen transverse sections were immunostained with a combination of anti-K15 (Lab Vision, Clone LHK15, 1:1,500 in antibody buffer) and anti-Desmin (Dako, Clone D33, 1:500 in antibody buffer) antibodies every 10^{th} slide according to established methods (1). Fluorescent-labeled,

isotype-specific secondary antibodies were used. The interfollicular epidermis was K15-negative (**Figure S1a**). Although the biopsies were cut in transverse orientation, the margins of the sections containing interfollicular epidermis contracted during OCT embedding, and became curved (~90 degree angle) as compared to the center of the tissue sample. This occurred since it was impossible to mount the tissue perfectly flat; as a result, the margins containing interfollicular epidermis appeared in vertical (longitudinal) orientation (as seen in **Figures 2a**, **S2a** and **S2c**). The hair follicle bulge exhibited strong K15 expression (**Figure S1b**), and it was defined as beginning at the insertion of the sebaceous gland duct and ending at the attachment of the desmin-postive arrector pili muscle (APM). By analyzing every 10^{th} slide, tissue samples in the intervening slides that contained cross-sections of hair follicle bulges could be targeted for F-LCM.

NKI-beteb expression in normal human skin

In order to determine the co-expression pattern of the NKI-beteb antibody (Cell Sciences, 1:10 in antibody buffer) with either TYR or DCT in the normal human hair follicle and epidermis, we combined it with either anti-TYR (Abcam, Clone T311, 1:10 in antibody buffer) or anti-DCT (Santa Cruz, Clone C-9, 1:100 in antibody buffer) antibodies as well as with an anti-K14 antibody (Lifespan Biosciences, 1:350 in antibody buffer) to identify surrounding KCs, using standard triple immunostaining procedures (2). We used an antibody buffer containing phosphate buffered saline with 10% normal goat serum, 2% bovine serum albumin, and 0.05% Tween-20. We used a combination of isotype-specific fluorescently-labeled secondary antibodies to bind to NKI-Beteb (Life Technologies, Goat Anti-Mouse IgG2b Alexa Fluor 488), DCT and TYR (Life

Technologies, Goat Anti-Mouse IgG2a Alexa Fluor 594), and K14 (Goat anti-Guinea Pig DyLight 350). Results were analyzed on a Nikon E400 fluorescent microscope and images were captured using a Nikon DS-QI1 camera and NIS Elements software (Nikon Instruments). Negative controls stained without primary antibodies were immunonegative.

Rapid Fluorescent Immunostaining for LCM

Frozen sections were immunostained using the mouse monoclonal NKI-beteb antibody (Cell Sciences, 1:5 in phosphate-buffered saline), to label immature and mature MCs in the epidermis and hair follicle bulge. Of different MC antibodies tested (anti-c-KIT, anti-PAX3, anti-DCT, NKI-beteb), NKI-beteb showed by far the strongest intensity after 20 minutes incubation. Some of these antibodies could show some staining at 1 and 2 hours, however, at these time-points, the RNA degradation was significant. For the immunostaining with NKI-antibody, we used an Alexa Fluor® 488 goat anti-mouse IgG (H+L) secondary Ab (Life Technologies, 1:100 in phosphate-buffered saline) and nuclease-free buffers from the HistoGene® LCM Frozen Section Staining Kit (Life Technologies). To further prevent RNA degradation, we added GeneAmp® RNAse-inhibitor (Life Technologies) to Ab dilutions in PBS.

Briefly, rapid immunostaining was conducted on copper blocks that were maintained at 4°C (3) (**Figure 1b-i)**. Slides were incubated for 10 minutes with primary antibody on the cold copper block, followed by secondary Ab incubation for a further 10 minutes on the cold copper block. All intervening washes were 30 seconds long, and conducted in nuclease-free buffers maintained at 4°C. Slides were dehydrated in an ethanol series, followed by xylenes and dried for 5 minutes at room temperature.

Fluorescent Laser Capture Microdissection

Laser capture was performed on slides within 1 hour of completing immunostaining. We used an infrared laser (Arcturus XTTM) microdissection system, under direct fluorescent microscopic visualization, in the LCM Core at the University of Colorado. We used the number of laser pulses (spot size = 16 μm) as an approximation of cell number collected for each sample. From each NBUVB-treated vitiligo and normal skin tissue sample, we captured 100 melanocytes (MCs) exhibiting fluorescent NKI-beteb antibody expression in the interfollicular epidermis (NKI-beteb positive cells exemplified in the figure 2a), another 100 positive cells from the hair follicle bulge (NKI-beteb positive cells exemplified in the **Figure 2b**), and 100 adjacent keratinocytes (KCs) (NKI-beteb negative) from each region. Depigmented vitiligo skin is devoid of epidermal MCs, so from this skin category we could not capture MC samples from the epidermis. However, we were able to capture MC samples from the bulge of depigmented vitiligo skin, since MCs are preserved in the bulge of this skin type (2). Cells on laser capture caps were lysed immediately in extraction buffer from the ARCTURUS® PicoPure® RNA Isolation Kit (Life Technologies), heated for 30 minutes at 42°C, and frozen at -80°C for further processing.

RNA Extraction, Amplification, qRT-PCR and statistical analysis

Total RNA was extracted from frozen LCM lysates using the ARCTURUS® PicoPure® RNA Isolation Kit (Life Technologies), and we obtained around 1-5 ng of total RNA per sample of 100 cells, eluted in 11 μL. Since it was often impossible to capture 100 cells on a single LCM cap, lysates from different caps were combined during the extraction process to produce complete samples from 100 captured cells. We

added an RNAse-free DNAse (Qiagen Inc.) digestion step to the RNA purification protocol, according to the recommendations listed in the RNA isolation kit. The quality of total RNA extracted from tissue scraped from slides used in LCM was assessed in the LCM core using an Agilent 2100 Bioanalyzer, and RNA integrity numbers averaged > 5.

Two different commercially-available kits were used to amplify total RNA from captured MCs and KCs. First, we amplified F-LCM samples from the skin of six NBUVB-treated vitiligo patients, which included samples of 100 MC and 100 adjacent KC from both the IE and the hair follicle bulge of each patient, using the Ovation RNA-Seq System V2 (NuGEN Technologies). Each purified RNA sample was split into two, 5 µL amplification reactions. We then combined resulting amplified SPIA cDNA during the final purification step, quantified cDNA samples using a NanoDrop 8000 spectrophotometer, and proceeded directly with qRT-PCR. These cDNA samples were used to analyze enrichment of MC and KC material presented in **Figure~~s~~ 3a**, and remaining cDNA was reserved for use in future whole transcriptome RNA sequencing studies.

As a comparison, we amplified separate F-LCM samples (100 MC from the interfollicular epidermis; 100 MC from the hair follicle bulge) from the skin of ~~four~~ six untreated vitiligo patients (bulge MC only), seven NBUVB-treated vitiligo patients (interfollicular epidermis MC and bulge MC), and six normal control patients (interfollicular epidermis MC and bulge MC) through two rounds using the Arcturus RiboAmp HS PLUS Kit (Applied Biosystems). Resulting antisense (a)RNA was quantified using a NanoDrop 8000 spectrophotometer, and 500 ng from each amplified sample was reverse transcribed using the QuantiTect Reverse Transcription Kit

(Qiagen), which includes a step to remove genomic DNA. The resulting cDNA samples using this method of amplification were used to analyze the stem-cell signature of the hair follicle bulge, presented in **Figures 3b, 3c,** and **S4**.

A total of 2 ng of cDNA (produced from either amplification protocol) was used for qRT-PCR using the QuantiTect SYBR® Green PCR Kit (Qiagen) and primers designed by ourselves. Primer pairs were designed using Primer3 (http://biotools.umassmed.edu/bioapps/primer3_www.cgi), and sequences are shown in **Supplementary Table S1**. To assess MC gene enrichment, we chose *TYR*, *DCT*, *TYRP1*, and *PMEL*, which are well-known MC-specific genes. To assess KC gene enrichment, we chose *KRT5* and *KRT14*, two KC-specific genes shown to be expressed in the basal layer of the interfollicular epidermis (4) and the hair follicle outer root sheath (5). To assess the MC samples captured in the hair follicle bulge for expression of stem cell genes, we chose *SOX9* (6, 7) and *ALDH1A1* (8, 9), since they have been shown to be involved in epithelial stem cell maintenance. We also analyzed expression of *WIF1* and *SFRP1* which have both been shown to be expressed by MC stem cells (10), and *ALCAM,* which has been shown to be expressed by human melanoma stem cells (11). qRT-PCR was performed on MX3000p and Aria-Mx real-time detection systems, and expression values were calculated using the standard delta Ct method normalized to B-Actin expression for each sample, using Ct=40 as a maximum value for samples that failed to reach the threshold. For example, not all stem-cell genes amplified in RNA samples from the interfollicular epidermis, so in those cases, maximum values of Ct=40 were used to estimate reduced fold expression levels compared to the bulge, and perform *t*-Tests.

Relative expression comparing different samples was calculated using the $2^{-\Delta\Delta C_T}$ method. Paired *t*-Tests were used to compare the average delta Ct values for samples that originated from the melanocyte versus keratinocyte capture of single patient sources (Figure 3a-black stars) or from interfollicular epidermis versus bulge of single patient sources (Figures 3b-black stars, 3c-black stars), using at least two replicate experiments. Unpaired *t*-Tests were used to compare the average delta Ct values for samples that originated from different skin types (interfollicular epidermis of NBUVB-treated vitiligo versus normal control interfollicular epidermis) (Figures 3b-red stars, 3ciii-red star) using at least two replicate experiments. Significance was determined using two-tailed analyses with $P < 0.05$.

The differences in expression for each gene transcript in the bulge melanocyte capture for all three groups (normal skin, untreated vitiligo skin, and NBUVB-treated vitiligo skin) were analyzed with one-way ANOVA followed by Tukey's test for multiple comparisons (GraphPad Prism 6 software), to generate adjusted P-values for all pairwise comparisons. Statistical significance was defined as adjusted *P*-value < 0.05.

SUPPLEMENTARY TABLES AND FIGURES

Figure S1. Bulge mapping. Frozen transverse sections immunostained with a combination of anti-K15 antibody (green), anti-Desmin antibody (red), and DAPI (blue), showing K15-negative interfollicular epidermis (**Panel a**), and strong signal (K15-positive) in the bulge ORS (**Panel b**). White scale bars: 100 μm.

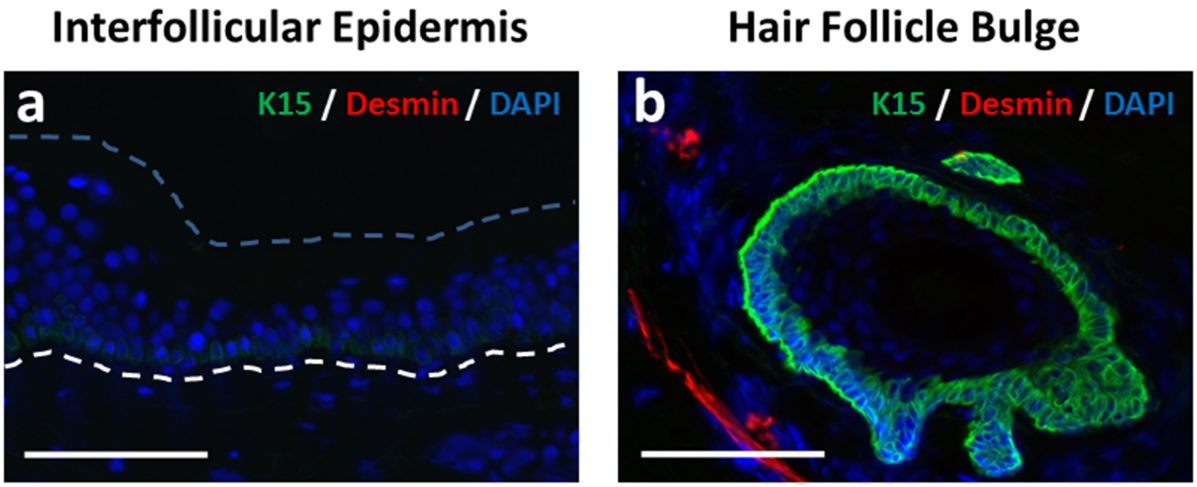

Figure S2. Expression of NKI-beteb in the normal human epidermis and hair follicle bulge. Transverse frozen sections of normal human skin immunostained with NKI-beteb (green), TYR (red), and K14 (blue), showing concomitant expression (yellow arrows) of TYR (red arrows) with NKI-beteb (green arrows) in the epidermal basal layer (**Panel a**) and NKI-beteb positive, but TYR negative cells in the bulge outer root sheath (**Panel b**, green arrows). Transverse sections of normal human skin immunostained with NKI-beteb (green), DCT (red), and K14 (blue), showing concomitant expression (yellow arrows) of DCT (red arrows) with NKI-beteb (green arrows) in the epidermal basal layer (**Panel c**) and bulge outer root sheath (**Panel d**). White scale bars: 100 μm for all panels.

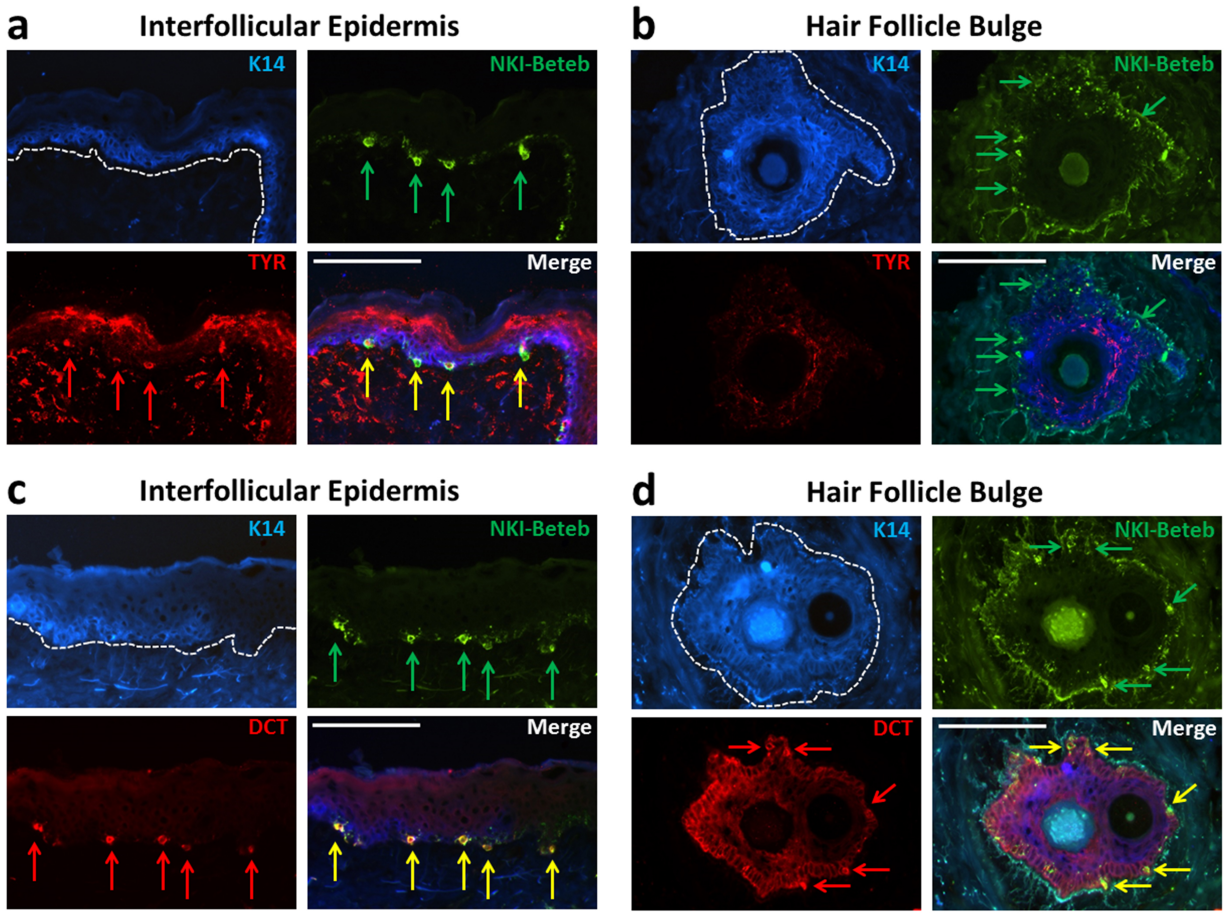

Figure S3. Cartoon example of fluorescent laser capture microdissection (F-LCM) technique. Melanocytes (MC) and keratinocytes (KC) capture is shown in the interfollicular epidermis (i) and hair follicle bulge (ii) with red circles indicating areas targeted by the laser spot. The capture was enriched in target cells, but could contain modest amounts of neighbor tissue (KC material for MC capture and MC dendrites for KC capture).

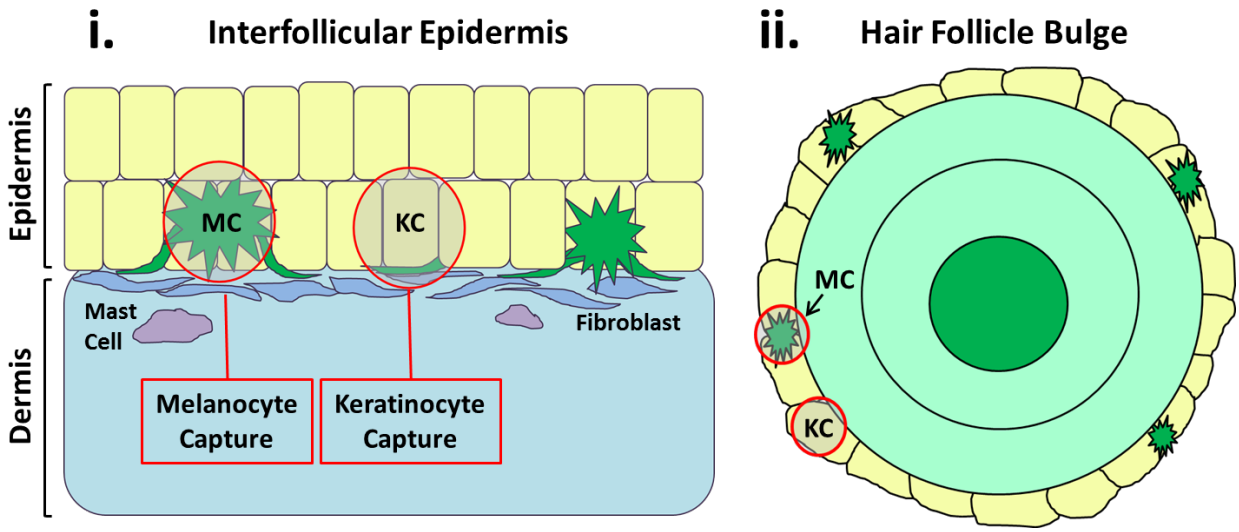

Figure S4. qRT-PCR analysis of melanocyte (MC) samples from Fluorescent Laser Capture Microdissection (F-LCM) in the bulge of untreated vitiligo, NBUVB-treated vitiligo and normal control skin.

F-LCM samples of 100 MC from the hair follicle bulge of 6 untreated vitiligo patients, 7 NBUVB-treated vitiligo patients and 6 normal control patients were amplified using the Arcturus RiboAmp HS PLUS Kit (Applied Biosystems) and subjected to qRT-PCR analysis of MC-specific genes (*TYR*, *DCT*, *TYRP1* and *PMEL*). The expression values of all 4 MC-specific gene transcripts were not significantly different (adjusted P >0.05, one-way ANOVA followed by Tukey's test for multiple comparisons), being maximal in the treated bulge, and minimal in the untreated bulge. Fold changes were set to 1 for MC samples from the untreated vitiligo bulge and were compared with expression values in the treated vitiligo bulge and in the normal control skin bulge.

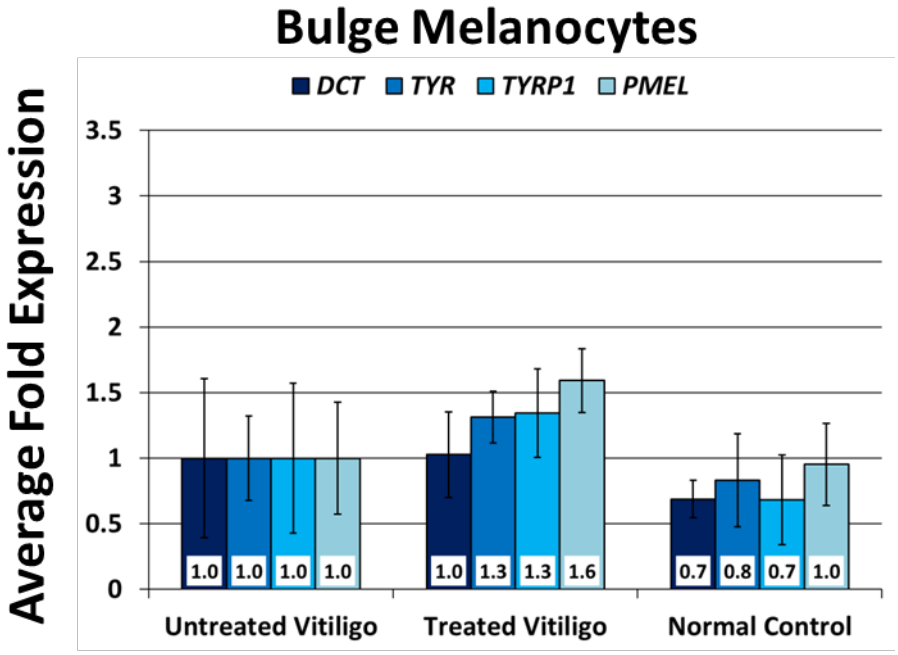

Table S1: Primer sequences used for qRT-PCR.

Primer	Sequence (5' – 3')	T_m (°C)	Prod. Size
***ACTB* Forward**	GAAGTCCCTTGCCATCCTAA	59.1	88 bp
***ACTB* Reverse**	TATCACCTCCCCTGTGTGG	59.3	
***TYR* Forward**	AGTGTAGCCTTCTTCCAACTCAG	59.1	126 bp
***TYR* Reverse**	TTCCTCATTACCAAATAGCATCC	59.4	
***DCT* Forward**	GCAGCAAGAGATACACAGAAGAA	58.8	95 bp
***DCT* Reverse**	TCCTTTATTGTCAGCGTCAGA	58.5	
***TYRP1* Forward**	AAGGCTACAACAAAAATCACCAT	59.0	115 bp
***TYRP1* Reverse**	ATTGAGAGGCAGGGAAACAC	59.1	
***PMEL* Forward**	ACTTCTCCGTACCCCAGTTG	59.1	147 bp
***PMEL* Reverse**	CCAGGAAAATCACAGCATCA	59.6	
***KRT5* Forward**	TTCTTTGGTTCCCAGGAGAG	59.3	161 bp
***KRT5* Reverse**	TGGGGATTCTGTTTTGATGA	58.9	
***KRT14* Forward**	TCTCCTCCTCCCAGTTCTCC	60.7	149 bp
***KRT14* Reverse**	GCAGCCTCAGTTCTTGGTG	59.6	
***ALDH1A1* Forward**	AATGTGACCCCCAAGTCCTA	59.3	156 bp
***ALDH1A1* Reverse**	AAGGGAAAGAAGCTAAATGCAA	59.4	
***SOX9* Forward**	TTTCCTCAAAGGGTATGGTCA	59.4	159 bp
***SOX9* Reverse**	AAAAAGGGATGGACAAAAAGG	59.3	
***WIF1* Forward**	ATTTTCAGTGTGTAGTTGGCAGAT	59.1	125 bp
***WIF1* Reverse**	GCACCATCCAAATTCTTGTG	59.0	
***SFRP1* Forward**	CCTGTGGGTTAGCATCAAGTT	59.1	100 bp
***SFRP1* Reverse**	TAGGTTTGGGAAATGGGATTAC	59.1	
***ALCAM* Forward**	CTCTGGACCGAAAGCAGAA	59.1	170 bp
***ALCAM* Reverse**	GAGAGCCGAAACCTCAAAAG	59.1	

SUPPLEMENTARY REFERENCES

1. Ohyama M, Terunuma A, Vogel JC. J Clin Invest 2006: 116: 249-260.
2. Goldstein NB, Koster MI, Hoaglin LG, *et al.* J Invest Dermatol 2015: 135: 2068-76.
3. Shellman YG, Ribble D, Yi M, *et al.* BioTechniques 2004: 36: 968-976.
4. Alam H, Sehgal L, Kundu S, *et al.* Mol Biol Cell 2011: 22: 4068-78.
5. Stark HJ, Breitkreutz D, Limat A, *et al.* Differentiation 1987: 35: 236–248.
6. Kadaja M, Keyes BE, Lin M, *et al.* Genes and Development 2014: 28: 328–341.
7. Vidal V, Chaboissier MC, Lützkendorf S, *et al.* Current Biology 2005: 15: 1340–1351.
8. Marchitti SA, Brocker C, Stagos D, *et al.* Expert Opin Drug Metab Toxicol 2008: 4: 697–720.
9. Chen Y, Koppaka V, Thompson DC, *et al.* Exp Eye Res 2012: 102: 105–106.
10. Lang D, Mascarenhas JB, Shea CR. Clin Dermatol 2013: 31:166–178.
11. Klein WM, Wu BP, Zhao S, *et al.* Mod Pathol 2007: 20: 102–107.